Global Journal of Engineering Convergence and Emerging Technologies (GJECET)
Abbreviated Key Title: Glob. J. Eng. Converg. Emerg. Technol.
ISSN 3156-271X. Open Access
Volume-2 (Issue): 11, November, Pp. 44-62, 2026
https://doi.org/10.5281/zenodo.24430912

Engineering Research Paper

RSM–ANN-Based Prediction of Chip Reduction Coefficient for Chip Evacuation and Tool-Life Improvement in Dry Drilling

Kingsley Udoka Enuezie[1], Jephthah Ikimi[2], Rilwan Omogbolahan Anjorin[3]

[1]Department of Mechanical Engineering, Maranatha University, Lagos, Nigeria.
[2]Department of Mechanical Engineering, Petroleum Training Institute, Effurun, Nigeria.
[3]Institute of Engineering, Technology & Innovation Management, University of Port Harcourt, Choba, Nigeria.

kenuezie@gmail.com, ikimi_ja@pti.edu.ng, rilwanoanjorin@gmail.com

Abstract

Chip removal is a critical factor in determining tool life in dry drilling, yet the chip reduction coefficient (CRC) which is a direct measure of chip removal remains underutilized in predictive process models. The present study develops and validates predictive models for CRC using Response Surface Methodology (RSM) as well as Artificial Neural Networks (ANN). Three input parameters (feed rate (0.03–0.37 mm/rev), cutting speed (106.36–173.64 m/min), and depth of cut (0.33–1.17 mm)) were investigated using a central composite design on mild steel workpieces. The 2nd order polynomial RSM model demonstrated excellent predictive capacity with R^2 of 0.9513, Adj. R^2 of 0.9075, and Adeq Precision of 15.603. ANOVA revealed that the interaction between feed rate and depth of cut (AC) was the most dominant factor ($F = 60.32$, $p < 0.0001$), followed by the quadratic effect of depth of cut (C^2: $F = 87.63$, $p < 0.0001$). Numerical optimization yielded an optimal CRC of 1.80833 at feed rate 0.30 mm/rev, cutting speed 146.22 m/min, and depth of cut 0.50 mm, with a desirability of 93.1%. ANN achieved R^2 of 85.15% (Exp = 0.1264 + 0.8884 ANN). The models presented provide industry-ready tools for predicting chip morphology and optimizing parameters to prevent chip clogging and subsequent tool breakage.

Keywords: Chip Reduction Coefficient, Dry Drilling, Tool Breakage, Chip Evacuation, Response Surface Methodology, Artificial Neural Network

Received 19/10/2026 Accepted 10/11/2026 Published 21/11/2026

1. INTRODUCTION

Machining is widely used for finalizing finishing operation for parts produced by casting and forming before they are ready for assemblage or usage. The evidence of material removal is usually the chip in most machining operation [1]. Additionally, precision and automation are strictly required in high-end manufacturing. Chip control provides an incredibly serious problem in the machining process. The geometry, thickness, and continuity of the chip is directly proportional to the efficiency and stability of the cutting process [2]. In dry drilling, where there is no cutting fluid to lubricate the tool-chip interface or assist chip evacuation, chip characteristics become magnified in their importance. Long, continuous chips which are typical of ductile materials like mild steel, tend to wrap around the drill bit, obstruct the flutes, and generate sudden spikes in torque [3,4]. The torque surges typically occur for fractions of a second before catastrophic tool failure, giving the operator and machine control system little warning. Chip reduction coefficient (CRC) expresses the extent of chip deformation through the relationship between the final chip thickness and its original thickness before machining.

Larger values indicate greater plastic distortion, often accompanied by reduced chip fragmentation, intensified friction, and elevated cutting temperatures. On the other hand, a low CRC implies smooth flow of the chip and a high possibility of the chip breaking into manageable segments [5,6]. Thus, CRC is not only a post-process evaluation of the risk of tool failure, but a predictor of it. The increasing interest in dry drilling has been urged by environmental regulations, high costs for cutting fluid disposal and the health risks of fluid mist inhalation [7,8]. However, the absence of coolant results in loss of heat dissipation and chip lubrication. Consequently, the coefficient of friction increases and the CRC [9,10] rises because chips stick more to the rake face. For deep-hole drilling, these effects multiply as chips generated at the cutting edge must be carried all the way down the flute into the deep hole, and the more chips that accumulate, the greater the resistance [11]. Once the CRC value is above a certain threshold, a clog will be formed, torque increases rapidly, and the drill will fracture, sometimes in seconds. Despite these well-documented failure mechanisms, most drilling optimization studies focus on cutting forces, feed forces or surface roughness, neglecting CRC as a primary response variable [12–14]. The present study fills this void by integrating the CRC into the optimization framework and directly relating chip deformations to the risk of tool breakage It seeks to formulate and evaluate RSM and ANN approaches for estimating CRC under dry-drilling conditions, considering feed rate, cutting speed, and depth of cut as the governing machining parameters. A secondary goal is to determine the best operating parameters, that is, those which result in the lowest CRC, and thus reduce the likelihood of tool breakage at suitable rates of material removal. Recent studies have demonstrated the applicability of machine learning and statistical modelling to chip-related responses and machining performance. Mishra et al., 2025 employed a Levenberg–Marquardt backpropagation artificial neural network (LM-ANN) to predict the chip reduction coefficient (CRC) and von Mises stress during dry turning of EN36C steel. The developed ANN achieved a high correlation coefficient and a very low CRC prediction error. Prashanth & Hiremath, (2023) applied generalized regression neural network (GRNN), adaptive neuro-fuzzy inference system (ANFIS), and regression analysis to predict thrust force, burr height, and radial overcut during dry micro-drilling of commercially pure titanium. The GRNN achieved the best performance, however, the investigated responses were primarily drilling force and hole-quality characteristics rather than CRC. Xu et al., (2021) developed a support vector regression model using sequential minimal optimization to predict axial drilling force during internal chip-removal drilling of CFRP. The model achieved close agreement between predicted and experimental drilling-force distribution; however, it focused on drilling force rather than chip deformation through CRC.

Previous studies in literature demonstrate the effectiveness of ANN, RSM, and other machine-learning approaches for predicting machining responses and optimizing chip-related processes. However, the studies predominantly address cutting force, drilling force, surface roughness, chip evacuation, and related chip characteristics, while limited attention has been given to CRC as a direct measure of chip deformation in dry drilling. Therefore, the present study addresses this gap by developing RSM and ANN independent models for predicting and optimizing CRC in dry drilling. The main contributions of the present study are summarized as follows:

(i) Investigation of CRC as a response for evaluating chip deformation during dry drilling, with particular emphasis on its relevance to identifying machining conditions associated with chip clogging and potential tool breakage.

(ii) Formulation and comparative assessment of RSM and ANN models for relating CRC to the principal drilling parameters, including feed rate, cutting speed, and depth of cut.

(iii) Determination of suitable drilling parameter combinations for reducing CRC through response-surface analysis and numerical optimization, while assessing the predictive capability of the developed ANN model as an alternative modelling approach.

The remainder of this paper is organized as follows. Section 2 describes the materials, experimental design, drilling parameters, RSM formulation, ANN architecture, and numerical optimization procedure. Section 3 presents the modelling results, analysis of variance, model adequacy assessment, residual diagnostics, interaction effects, optimization results, and ANN performance evaluation. Section 4 summarizes the major findings and concludes of the present study; with a brief statement of possible related research areas in this domain.

2. MATERIALS AND METHODS

2.1 Workpiece Material and Tooling

The experiments were carried out with mild steel specimens of size 100mm×400mm×50mm. The material was selected because of its extensive use in engineering and manufacturing, availability, and moderately low cost. However, owing to the interaction between the cutting tool and the workpiece material, mild steel has a tendency to form built-up edges during dry machining, which makes it less suited to industrial applications. With this feature and a moderate machinability, it is an appropriate material for research related to the mechanical and thermal conditions of tool failure in drilling operations. The drilling was carried out in a DT drilling machine with high-speed steel (HSS) twist drill. HSS were used due to their wide application in small and medium production sectors and their sensitivity

to excessive thermal loading and mechanical stresses, making them suitable for tool breakage assessment under different drilling conditions.

2.2 Experimental Design Using CCD, Central Composite Design

The experiment was structured around a three-factor Central Composite Design (CCD) to investigate the influence of drilling parameters on the measured responses. The design was considered appropriate because it accommodates both linear and nonlinear relationships between process variables and responses, while permitting the development of a second-order polynomial model without requiring an excessively large experimental dataset. In comparison with a basic factorial arrangement, CCD provides additional experimental points that enable the identification of response curvature and interaction effects. For the three investigated factors, the experimental matrix comprised 20 runs, consisting of eight factorial combinations generated from a 2^3arrangement, six axial experiments positioned at $\alpha = \pm 1.682$ and six replications at the design centre. The inclusion of repeated centre-point experiments served two purposes: establishing the experimental pure error and providing a basis for evaluating the adequacy of the fitted model through lack-of-fit assessment. Feed rate (A), cutting speed (B), and depth of cut (C) were defined as the independent variables. Each factor was investigated at five levels, corresponding to the coded values of −1.682, −1, 0, +1, and +1.682. The actual operating conditions associated with these coded levels are presented in Table 1.

Table 1: Machining Factors and their corresponding Experimental Settings

Machining Factor	Code	Unit	Lower axial point (−α)	Lower factorial level (-1)	Central design point (0)	Upper factorial level (+1)	Upper axial point (−α)
Feed rate	A	mm/rev	0.03	0.10	0.20	0.30	0.37
Cutting speed	B	m/min	106.36	120.00	140.00	160.00	173.64
Depth of cut	C	mm	0.33	0.50	0.75	1.00	1.17

2.3 Response Surface Methodology.

The experimental results were analysed using RSM in Design-Expert software (version 7.01). The modelling approach was adopted to quantify the relationship between the selected drilling conditions, presented in Table 1 as input features, and the resulting chip reduction coefficient. Its application provides an advantage over conventional one-factor-at-a-time experimentation by simultaneously examining the individual contributions of process variables, their combined effects, and nonlinear response behaviour. Consequently, the relationships governing the machining response can be evaluated with a relatively limited number of experimental observations.

Model development involved fitting a second-order polynomial regression equation to the experimental data to describe the behaviour of the response within the investigated operating ranges. The mathematical representation of the fitted model is given in Eqn. 1. [18], where Y represents the predicted strain on chip at time of breakage, $X_i \, and \, X_j$ denote the coded independent variables corresponding to feed rate, cutting speed, and depth of cut; β_0 is the constant term representing the model intercept; β_j represents the linear regression coefficients associated with the individual process parameters; β_{ij} describes the interaction coefficients, indicating the combined influence of two independent variables on the response; and β_{jj} denotes the quadratic coefficients responsible for accounting for curvature in the response surface. The term ε represents the random experimental error associated with the model.

$$Y = \beta_0 + \sum_{j=1}^{3} \beta_j X_j + \sum_{j=1}^{3} \beta_{jj} X_j^2 + \sum_{i<j}^{3} \sum \beta_{ij} X_i X_j + \mathcal{E} \quad (1)$$

The regression model was selected based on a comparative evaluation of the linear, 2FI, quadratic and cubic models using sequential sum of squares analysis. This statistical technique analyzes how much further explanatory power is provided when higher-order polynomial terms are added. The quadratic formulation was eventually used because the performance of the model was significantly enhanced when the formulation was added, compared to the alternative of 2FI ($p < 0.0001$). The cubic model had the highest predicted coefficient of determination (predicted R^2) and the lowest predicted residual error sum of squares (PRESS) however, this model was classified as aliased as there were not enough independent observations to estimate all the coefficients of the model. Following model selection, its statistical soundness was examined using several complementary assessment techniques. Sequential F-

tests were employed to establish the significance of the regression terms, while analysis of variance lack-of-fit tests determined whether the model adequately described the observed response patterns. A non-significant lack-of-fit was considered an indication of satisfactory model representation. The explanatory strength of the regression was quantified using the coefficient of determination (R^2), which indicates the fraction of total response variation accounted for by the model [19,20]. Adjusted R^2 was additionally considered to account for model complexity and discourage the retention of unnecessary terms, whereas predicted R^2, obtained using PRESS, provided an indication of the model's ability to predict unobserved responses. Adequate precision was also explored as a measure of the relationship between the predicted signal and associated noise, with values greater than 4 being considered sufficient predictive signal to explore the design space. The potential multicollinearity among the model terms was tested using variance inflation factors (VIF) with a value near 1.0 being the ideal situation. Also, regression assumptions were examined using graphical and statistical residual diagnostics. Normal probability plots of studentized residuals were used to assess residual normality, on the other hand, Cook's distance was used to identify observations with potentially excessive influence on the fitted model. The distribution of residuals was also examined to test error variance consistency. The final quadratic regression equation was written in terms of the actual values for the input variables, not their coded values, so as to make the relationship more easily applicable to manufacturing settings.

2.4 Artificial Neural Network

A feedforward ANN was implemented in MATLAB as an alternative modelling technique to complement the RSM framework. It was selected based on its ability to approximate functions universally, or to find a function that matches a set of data points without requiring knowledge of the underlying mathematical model [21,22]. The feature described makes ANN suitable for dry drilling analysis because thermal softening, strain hardening and chip clogging give rise to the nonlinear response behaviour. The network comprised three layers, with three input neurons representing feed rate, cutting speed, and depth of cut, a hidden layer containing 10 neurons with a log-sigmoid (logsig) activation function, and a single output neuron employing a linear (purelin) transfer function. The hidden-layer configuration was determined by trial-and-error testing with neurons ranging from 4 to 20, and 10 neurons were determined to be the optimum number that minimised validation error without overfitting. All experimental data were normalized using min–max normalization in the interval [0,1] before training, and the min–max parameters were calculated only for the training set, not for the test set, to avoid data leakage, and to reduce the effect of the magnitude difference of the variables on weight adjustments. The optimization algorithm used for the network was the Levenberg-Marquardt backpropagation algorithm due to its convergence efficiency and numerical stability over conventional gradient descent. An early stopping criterion stops training after 6 epochs of no improvement in validation error, thus preventing overfitting. Predictive performance was subsequently assessed using the independent testing dataset and established metrics, namely coefficient of determination (R^2) and mean squared error (MSE) [23–26] While RSM yields an interpretable quadratic expression, ANN offers greater flexibility in identifying subtle nonlinear patterns, although with reduced interpretability.

2.5 Numerical Optimization and Validation

The optimum drilling conditions were established through numerical optimization based on the desirability function technique, which converts the specified response objectives into a unified index ranging from 0 to 1. The optimization criterion was defined as minimizing the chip reduction coefficient, while feed rate, cutting speed, and depth of cut were constrained to their respective experimental limits. Among the generated solutions, the parameter combination associated with the highest desirability value was identified as the optimal operating condition. Experimental confirmation of the predicted optimum was outside the scope of the present investigation and is therefore recommended for subsequent studies.

3. RESULTS

3.1 Modelling and Optimization with Response Surface Methodology

Response Surface Methodology (RSM) was employed to investigate the effects of the selected machining parameters on the chip reduction coefficient and to establish their optimum combination. RSM offers a systematic statistical model for assessing the relationship between one or more responses and independent process variables and is extensively used for process development and optimization. The objective of optimization in the present study was to minimize the chip reduction coefficient by selecting appropriate values of feed rate, cutting speed and depth of cut. The experimental data required for the optimization were generated using a Design of Experiments (DOE) approach based on CCD. CCD is widely used for RSM based investigations because it offers an efficient approach to quadratic model development and

optimization of process conditions. The resulting experimental matrix consisted of twenty (20) runs, comprising eight (8) factorial points, six (6) axial points, and six (6) centre points. The experimental design and subsequent optimization analysis were carried out using Design-Expert software version 7.01. To assess the appropriateness of the second-order polynomial model for representing the experimental observations, the sequential model sum of squares was evaluated using the measured chip reduction coefficient. The corresponding results are presented in Table 2.

Table 2: Sequential statistical assessment of polynomial models for CRC prediction

Source	Sum of Squares	Df	Mean Square	F Value	p-value Prob > F	
Mean vs Total	18.74	1	18.74			
Linear vs Mean	0.13	3	0.043	0.13	0.9382	
2FI vs Linear	2.44	3	0.81	3.98	0.0326	
2^{nd} order vs 2FI	2.40	3	0.80	31.48	< 0.0001	Suggested
3^{rd} order vs 2^{nd} order	0.066	4	0.016	0.52	0.7229	Aliased
Residual	0.19	6	0.031			
Total	23.97	20	1.20			

The incremental contributions of the terms in the model to the overall goodness of fit were evaluated using the sequential sum of squares analysis. The polynomial order was selected based on the highest model degree for which the additional terms were statistically significant and the model remained unaliased. The third order polynomial was identified as aliased and was not included in the final predictive polynomial as shown in Table 2. The second-order model and two-factor interaction (2FI) were suggested as the best models; hence, the quadratic polynomial model was adopted for subsequent analysis. The validity of the selected second order model was further checked by the lack-of-fit test to ascertain if the model was adequate to represent the variation observed in the experimental data. A statistically significant lack of fit indicates that the model does not adequately describe the response and, therefore, should not be relied upon for prediction. The lack-of-fit results obtained for the chip reduction coefficient are presented in Table 3.

Table 3: Statistical evaluation of model adequacy using the lack-of-fit test for CRC

Model order	Sum of Squares	df	Mean Square	F Value	p-value Prob > F	
Linear	4.91	11	0.45	11.84	0.0068	
2FI	2.47	8	0.31	8.19	0.0165	
2^{nd} order	0.066	5	0.013	0.35	0.8627	Suggested
3^{rd} order	1.122×10^{-4}	1	1.122×10^{-4}	2.976×10^{-3}	0.9586	Aliased
Pure Error	0.19	5	0.038			

The results given in Table 3 show that the second order polynomial had a non-significant lack of fit and thus it was considered adequate for further model development and analysis. The third order polynomial, however, resulted in a major lack of fit and was deemed unsuitable and rejected for further modelling. Model standard error further assessed the appropriateness of RSM with the selected quadratic model for minimizing the chip reduction coefficient. The standard error values for the response has been calculated and reported in Table 4.

Table 4: Statistical Diagnostics of Individual Model Terms and their associated Standard Errors

Model Term	Standard Error	VIF	R-Squared	0.5 Std. Dev.	1 Std. Dev.	2 Std. Dev.
A	0.27	1.00	0.0000	13.3 %	38.6 %	91.4 %
B	0.27	1.00	0.0000	13.3 %	38.6 %	91.4 %
C	0.27	1.00	0.0000	13.3 %	38.6 %	91.4 %
AB	0.35	1.00	0.0000	9.8 %	24.9 %	72.2 %
AC	0.35	1.00	0.0000	9.8 %	24.9 %	72.2 %
BC	0.35	1.00	0.0000	9.8 %	24.9 %	72.2 %
A^2	0.26	1.02	0.0179	40.4 %	92.7 %	99.9 %
B^2	0.26	1.02	0.0179	40.4 %	92.7 %	99.9 %
C^2	0.26	1.02	0.0179	40.4 %	92.7 %	99.9 %

Results of the fitted model in Table 4 clearly show that the standard errors of individual coefficients, combined effects and second-order terms were 0.27, 0.35, and 0.26 respectively, which are relatively small. Since coefficients belonging to the same category are expected to have comparable standard errors, the relatively low values indicate satisfactory coefficient estimation. Furthermore, all the estimated errors were below the model standard deviation of 1.0, supporting the suitability of the quadratic RSM model for the optimization of the chip reduction coefficient. The variance inflation factor (VIF) values were also close to the ideal value of 1.0, indicating low multicollinearity between the model terms. VIF values that are greater than 10 are typically seen as a red flag as they may indicate that there are high correlations between predictors, which can produce unreliable coefficient estimates. Finally, the statistical significance and overall adequacy of the second-order polynomial model for minimizing the chip reduction coefficient was examined using Analysis of Variance (ANOVA) and the results are presented in Table 5.

Table 5: Statistical significance and adequacy evaluation of the CRC regression model

Source	Sum of Squares	Df	Mean Square	F Value	p-value Prob > F	
Model	4.97	9	0.55	21.71	< 0.0001	significant
A-feed rate	0.024	1	0.024	0.95	0.3526	
B-cutting speed	0.10	1	0.10	4.08	0.0710	
C-depth of cut	3.45×10^{-4}	1	3.45×10^{-4}	0.014	0.9096	
AB	0.25	1	0.25	9.69	0.0110	
AC	1.54	1	1.54	60.32	< 0.0001	
BC	0.66	1	0.66	25.86	0.0005	
A^2	0.079	1	0.079	3.09	0.1092	
B^2	0.053	1	0.053	2.10	0.1781	
C^2	2.23	1	2.23	87.63	< 0.0001	
Residual Error	0.25	10	0.025			
Lack of Fit	0.066	5	0.013	0.35	0.8627	not sig.
Pure Error	0.19	5	0.038			
Cor Total	5.23	19				

Analysis of variance (ANOVA) was used to ascertain the statistical significance and predictive adequacy of the developed regression model. The analysis also provided a means of determining the individual effects of the input variables, their interaction contributions, and the associated second-order polynomial terms on the response. The adequacy of the quadratic model in minimizing the chip reduction coefficient was also examined using goodness-of-fit and model adequacy statistics, as presented in Table 6.

Table 6: Model GOF Statistics for CRC Prediction

Statistical Indicator	Computed Value	Statistical Indicator	Computed Value
Standard Deviation	**0.16**	**R^2**	**0.9513**
Response Mean	0.97	Adjusted R^2	0.9075
Coefficient of Variation (%)	16.48	Predicted R^2	0.8506
PRESS	0.78	Adequate Precision	15.603

Table 6 presents the statistical indicators, which validate the developed model. The Predicted R^2 of 0.8506 shows reasonable agreement with the Adjusted R^2 of 0.9075, indicating that the model provides a satisfactory representation of the experimental response. The adequacy of the model was also supported by the adequate precision value that evaluates the signal-to-noise ratio. Since a ratio greater than 4 is considered desirable, the obtained value of 16.48 indicates a sufficiently strong signal relative to the noise. The results therefore demonstrate that the developed model is suitable for exploring the design space and determining conditions for minimizing the chip reduction coefficient. The optimization equation includes individual contributions of the process variables and interaction effects. The variables considered were feed rate, cutting speed, and depth of cut, with their effects on the experimentally measured chip reduction coefficient represented using actual factor values in Figure 1.

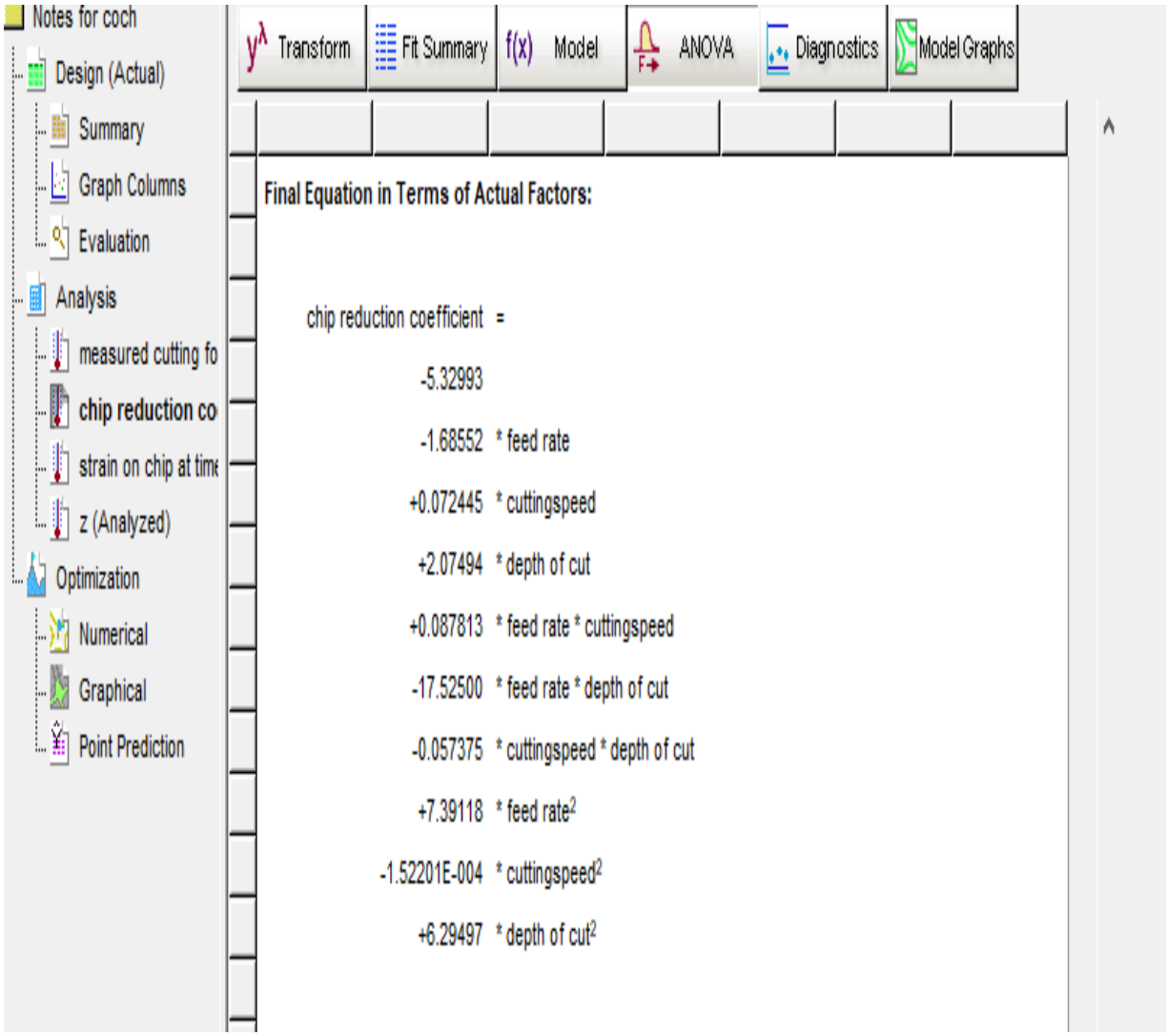


Figure 1. Optimal Equation in Terms of Actual Factors for Chip Reduction Coefficient

The comparison between experimentally measured CRC values and their corresponding model predictions is presented in Table 7.

Table 7: Diagnostics Case Statistics Report of Chip Reduction Coefficient

Standard Order	Actual Value	Predicted Value	Residual	Leverage	Internally Studentized Residual	Externally Studentized Residual	Influence on Fitted Value DFFITS	Cook's Distance	Run Order
1	0.40	0.42	-0.023	0.670	-0.255	-0.243	-0.345	0.013	19
2	1.10	1.03	0.067	0.670	0.736	0.718	1.022	0.110	8
3	0.90	0.82	0.080	0.670	0.870	0.858	1.222	0.153	20
4	2.20	2.13	0.068	0.670	0.742	0.724	1.031	0.112	15
5	1.80	1.86	-0.063	0.670	-0.691	-0.671	-0.956	0.097	17
6	0.65	0.72	-0.075	0.670	-0.818	-0.803	-1.144	0.136	10
7	1.05	1.11	-0.063	0.670	-0.684	-0.665	-0.947	0.095	1
8	0.70	0.67	0.028	0.670	0.306	0.292	0.416	0.019	4
9	0.87	0.83	0.044	0.607	0.437	0.419	0.521	0.030	13
10	0.92	0.97	-0.050	0.607	-0.504	-0.484	-0.602	0.039	16
11	0.43	0.37	0.058	0.607	0.583	0.563	0.700	0.053	6
12	0.60	0.67	-0.065	0.607	-0.650	-0.630	-0.784	0.065	14
13	1.70	1.81	-0.11	0.607	-1.118	-1.134	-1.410	0.193	11
14	1.90	1.79	0.11	0.607	1.051	1.057	1.315	0.171	7
15	0.95	0.69	0.26	0.166	1.811	2.096	0.936	0.065	12
16	0.62	0.69	-0.071	0.166	-0.484	-0.465	-0.208	0.005	18
17	0.47	0.69	-0.22	0.166	-1.514	-1.636	-0.731	0.046	5
18	0.65	0.69	-0.041	0.166	-0.278	-0.265	-0.118	0.002	2
19	0.55	0.69	-0.14	0.166	-0.965	-0.961	-0.429	0.019	3
20	0.90	0.69	0.21	0.166	1.438	1.531	0.684	0.041	9

The diagnostic results presented in Table 7 indicate satisfactory model fitting, as reflected by the relatively small residual values and corresponding leverage statistics. However, the reliability of the fitted model was further examined through statistical diagnostics to establish whether the underlying regression assumptions were adequately satisfied. Accordingly, the normal probability distribution of the residuals associated with the chip reduction coefficient was examined, as illustrated in Figure 2.

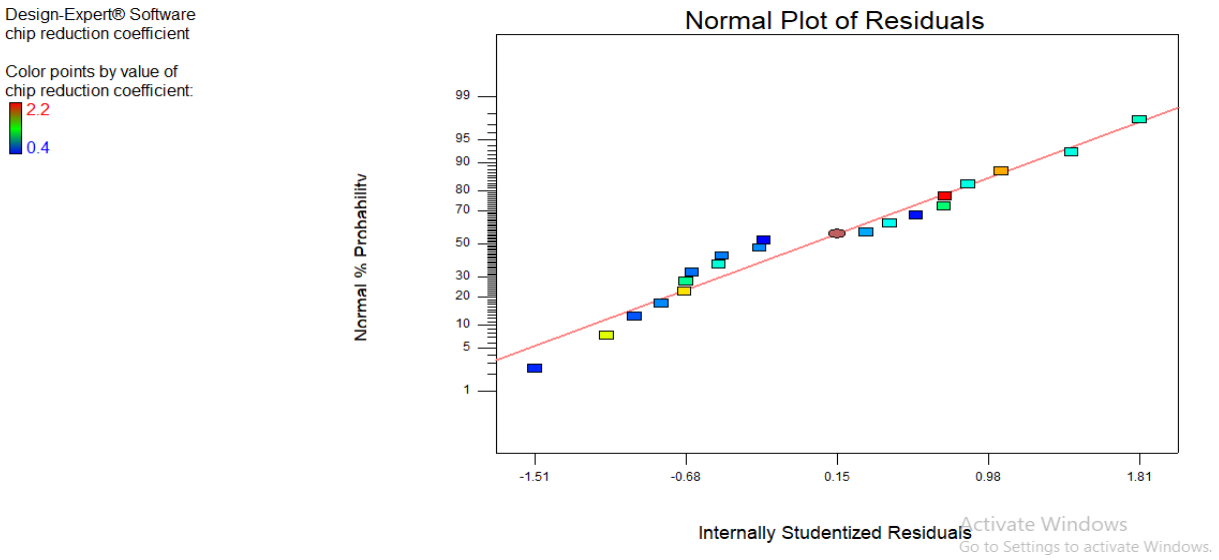


Figure 2. Distribution Pattern of Studentized Residuals in the CRC Regression Model

The normal probability plot of the studentized residuals was used to evaluate whether the residuals obtained from the developed model satisfy the assumption of normality. The residual is the difference between the observed and predicted response values and is shown as a percent of the standard deviation. Examination of the normal probability plot in Figure 2 shows that the residual points are distributed approximately along the expected normal trend, indicating that the residuals are reasonably normally distributed. This confirms the adequacy of the developed model and suggests that the dataset does not contain apparent abnormal observations that could adversely affect the model. To further examine the possibility of influential observations, Cook's distance was also evaluated. Cook's distance quantifies the extent to which the fitted regression model would be affected by the removal of an individual observation. An observation with a substantially larger Cook's distance than the remaining observations may exert undue influence on the regression model and therefore warrants further investigation. The resulting Cook's distance plot for the response is presented in Figure 3.

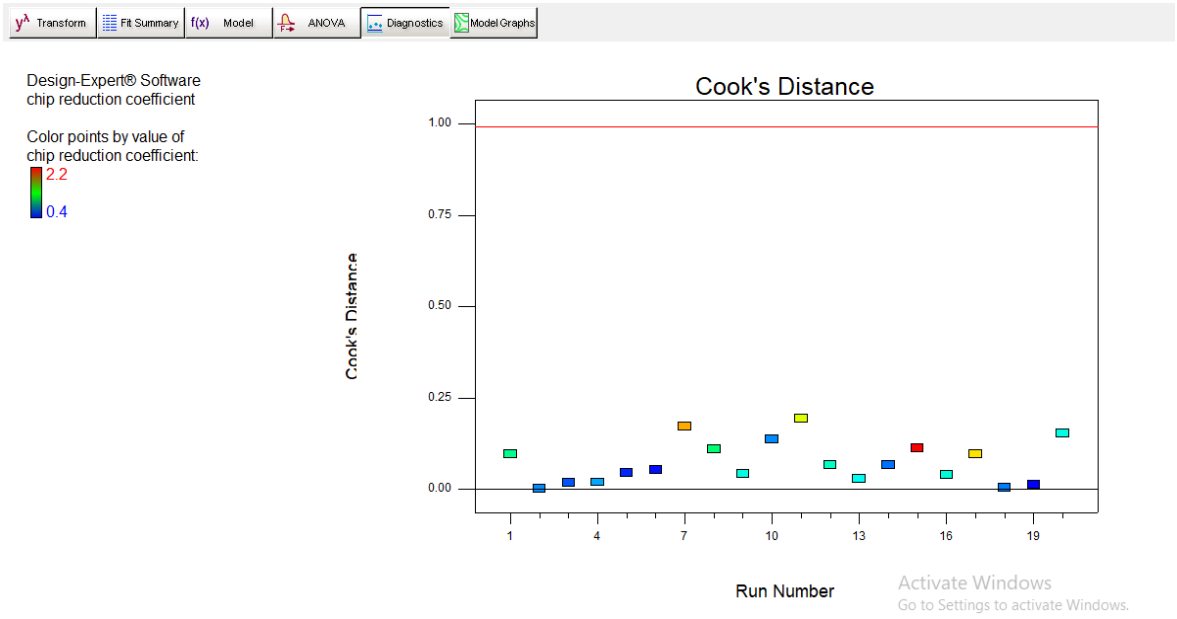


Figure 3. Generated Cook's Distance for Chip Reduction Coefficient

3D surface plots as presented in Figure 4 were used to study the effects of combine input variables on the response variable (chip reduction coefficient).

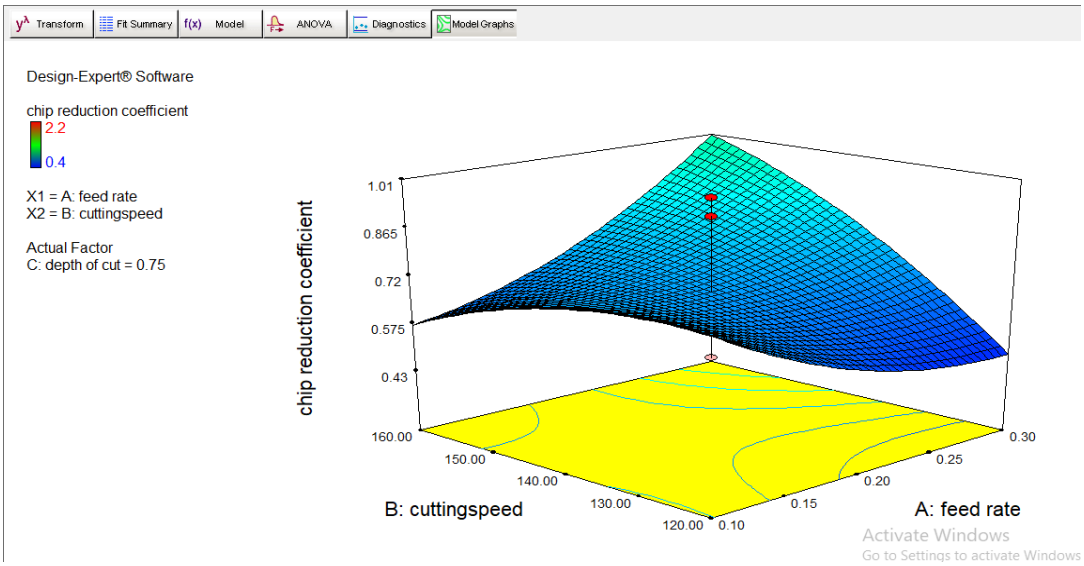


Figure 4. Three-Dimensional Surface Analysis of CRC Response to Cutting Speed and Feed Rate

3D surface plots as presented in Figure 5 were used to study the effects of combine input variables on the response variable (chip reduction coefficient).

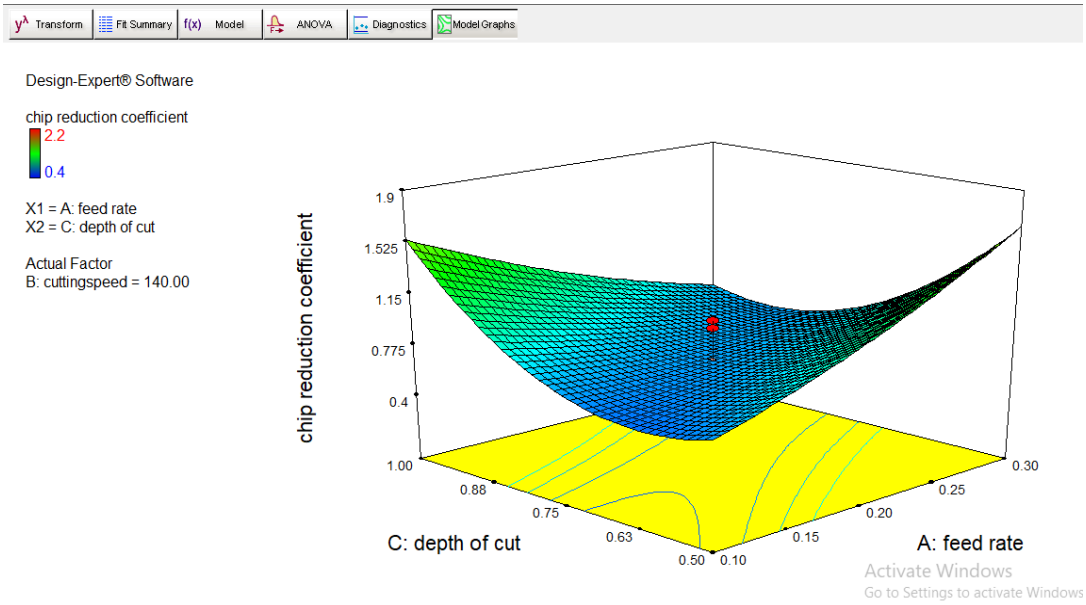


Figure 5. Three-Dimensional Surface Analysis of CRC Response to Feed Rate and Depth of Cut

3D surface plots as presented in Figure 6 were used to study the effects of combine input variables on the response variable (chip reduction coefficient).

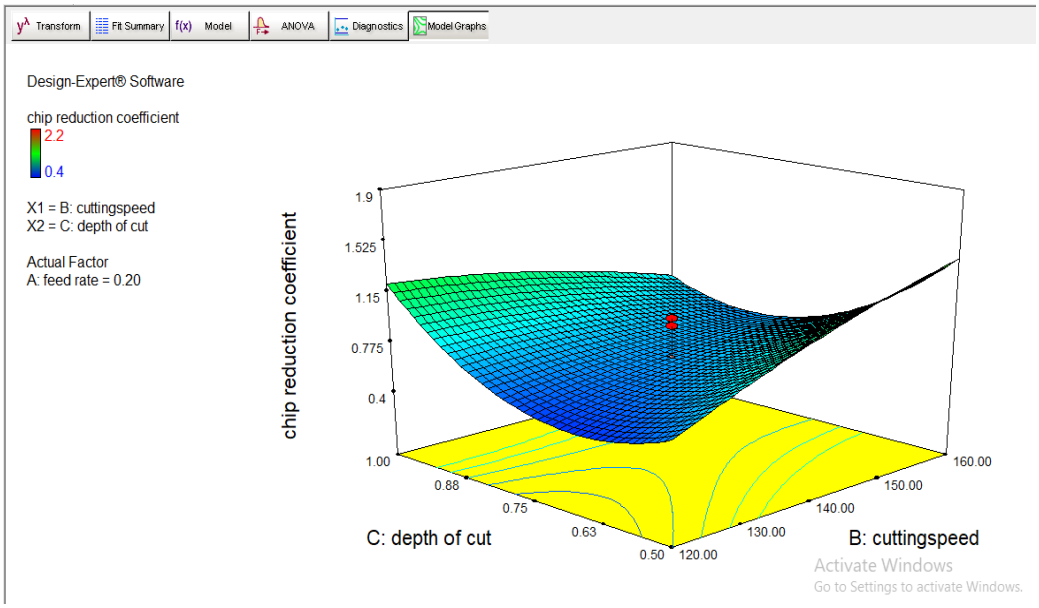


Figure 6. Three-Dimensional Surface Analysis of CRC Response to Depth of Cut and Cutting Speed

The overall suitability of the developed model was further investigated through numerical optimization to identify the operating conditions that yield the most desirable response. The optimization procedure sought to establish the optimal combination of current (A), voltage (V), and gas flow rate (L/min) for achieving the minimum chip reduction coefficient. The Design-Expert numerical optimization interface, illustrating the specified response objective and optimization criteria, is presented in Figure 7.

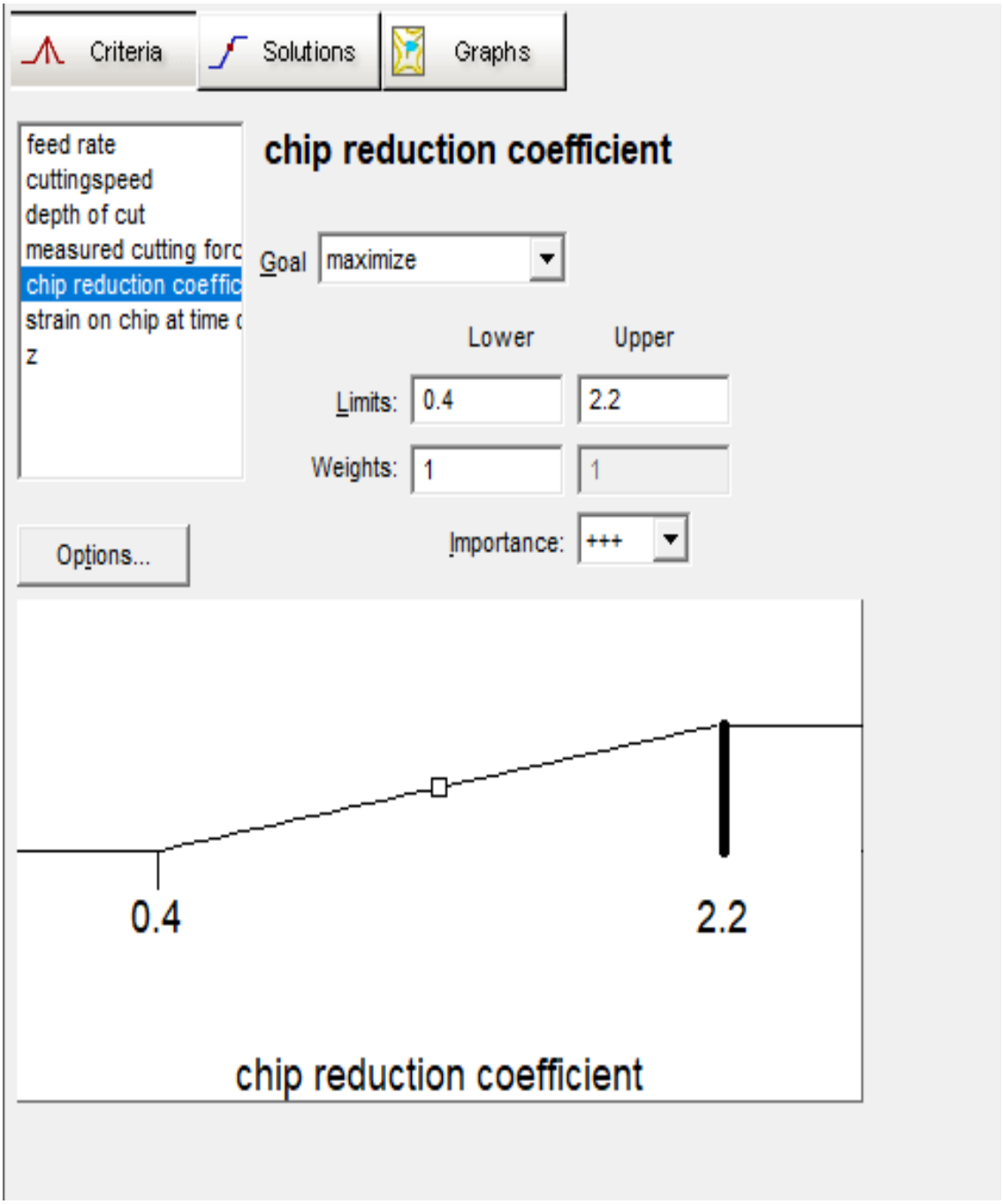


Figure 7. Percentage Dilution for Measured Chip Reduction Coefficient

The numerical optimization procedure was conducted with the aim of obtaining the minimum possible chip reduction coefficient. The response was given a relative importance value of 5.0, and its lower and upper limits for optimization were set at 0.1 and 1.0, respectively. The relevant boundary conditions are set to specify the acceptable range and to direct the optimization in the direction of the minimum value of the chip reduction coefficient. Once optimum operating conditions were determined, contour plots were created to show the relationship between the response and the optimized input parameters, as seen in Figures 8–10.

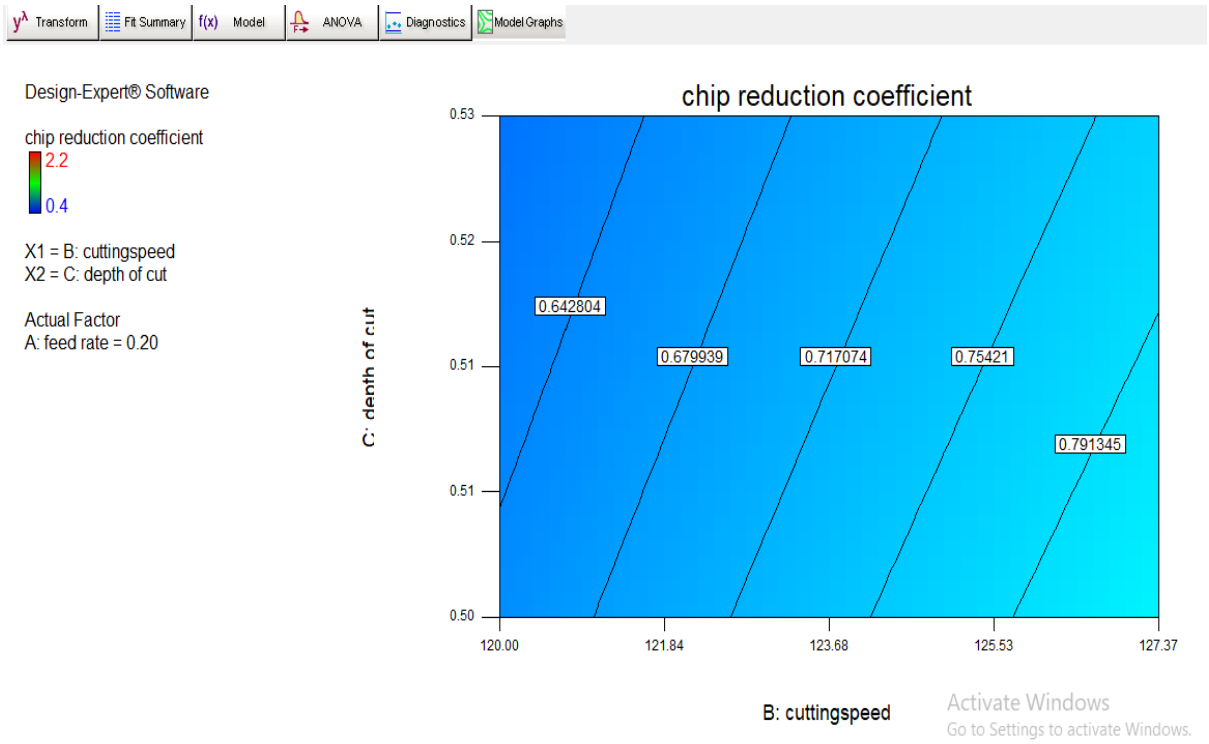


Figure 8. Contour-Based Analysis of CRC Response to Depth of Cut and Cutting Speed

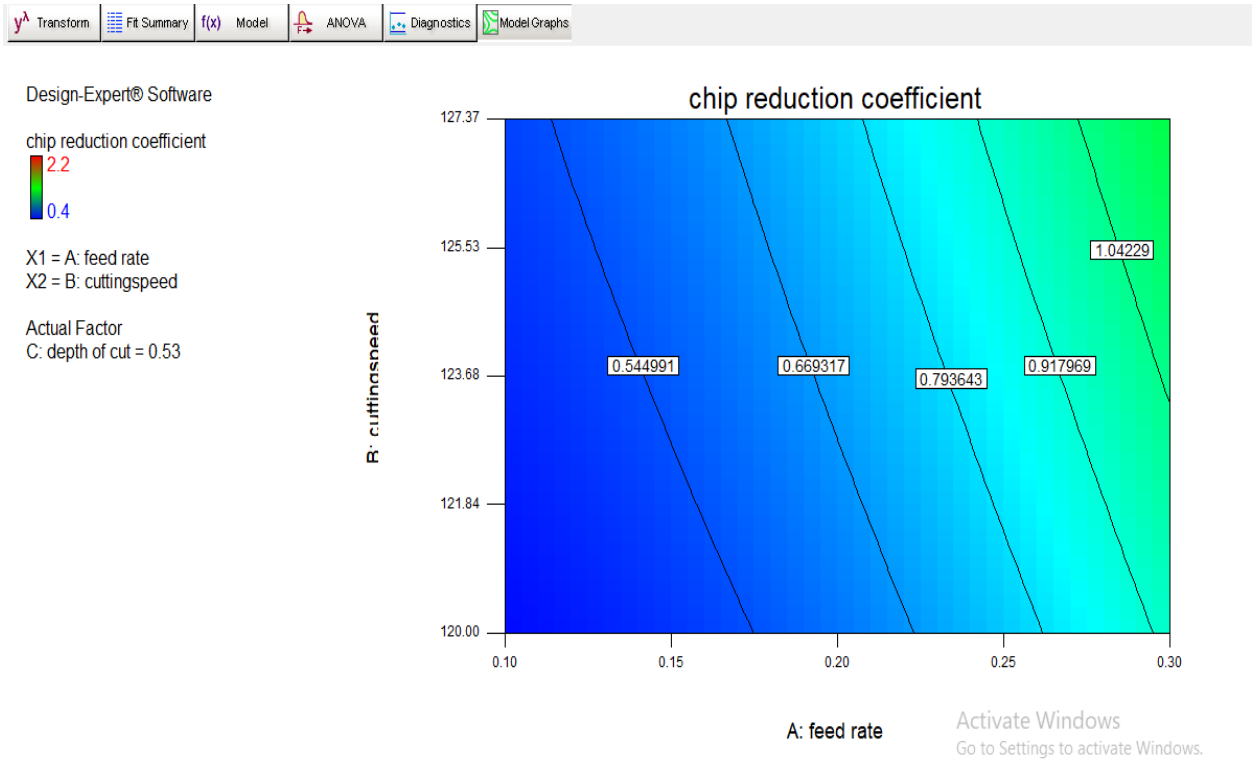


Figure 9. Contour-Based Analysis of CRC Response to Cutting Speed and Feed Rate

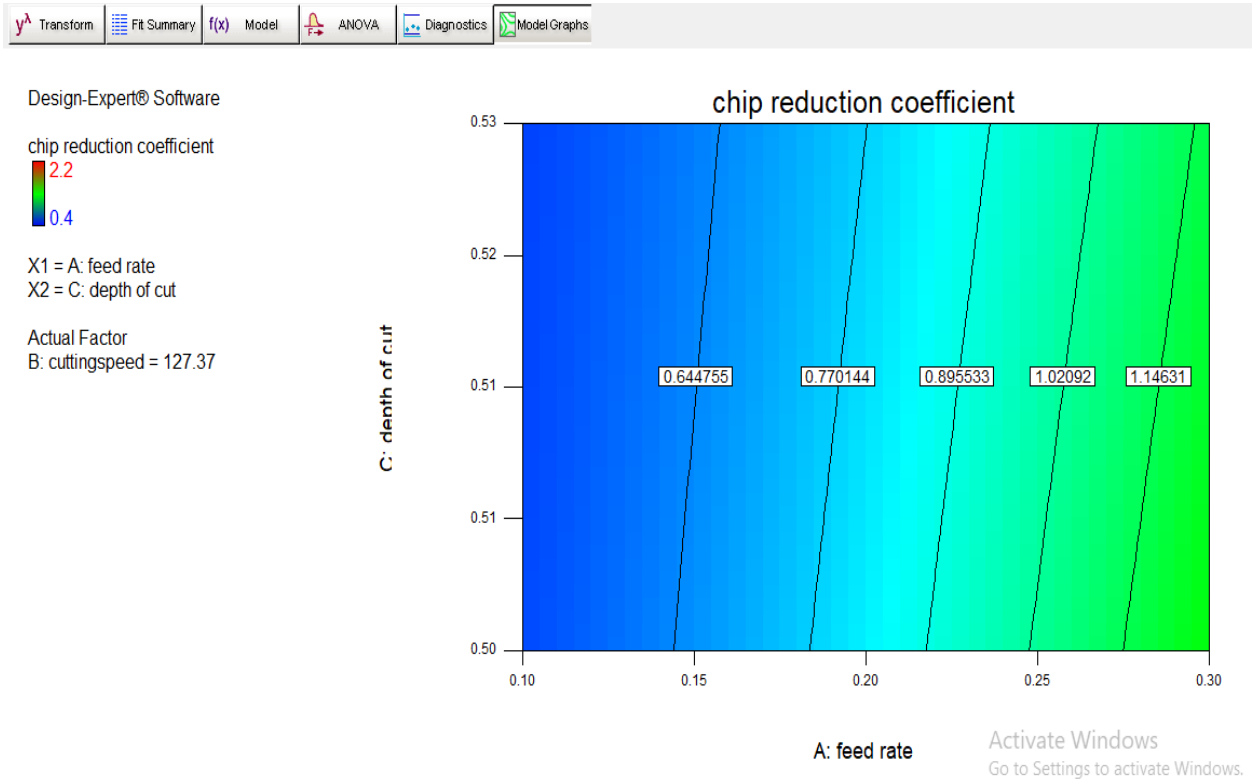


Figure 10. Contour-Based Analysis of CRC Response to Depth of Cut and Feed Rate

3.2 Modelling and prediction with Artificial Neural Network

The numerical optimization procedure based on Response Surface Methodology (RSM) successfully established the optimum combination of depth of cut, cutting speed, and feed rate for achieving a minimum chip reduction coefficient. Additionally, RSM furnished the mathematical model for the relationship between the process parameters selected and the associated response. The predictive capacity of RSM is closely linked to the quality and extent of the experimental design, however, and is therefore limited when predicting responses beyond the range of the experimental conditions studied. An Artificial Neural Network (ANN) model was thus used to offer an alternative solution to overcome this limitation and predict the responses beyond the experimental design space. Prior to ANN model development, the experimental observations were normalized to place the input variables on a comparable scale. This preprocessing step helped minimize variations in the magnitude of the network weights and supported stable network training, thereby reducing the likelihood of overtraining during the modelling process. Overtraining tends to focus the network on numerical values or sizes of the input instead of the physical relationship that makes up the process. The network properties and a portion of the raw experimental data are shown in Fig. 11, and the normalized version of the data used for training, validation, and testing are shown in Fig. 12. Figure 11 shows the network architecture and a portion of the raw data. The three input variables are designated as In1, In2, and In3, representing depth of cut, cutting speed and feed rate respectively. The measured chip reduction coefficient (out1) is the output variable. Figure 12 presents the data following transformation to a common scale, ensuring that the variance in depth of cut, cutting speed and feed rate contributes equally to the adjustment of network weights during the learning process. The neural network model was designed as a multi-layer, non-linear model that translates the interaction between the three parameters of electricity / flow (E, F, and E x F) and the resulting mechanical coefficient of chip reduction. Figure 12 also shows the overall structure of the network, consisting of the number of hidden layers, neurons in each layer, and chosen training algorithm that minimizes the prediction error of chip reduction coefficient.

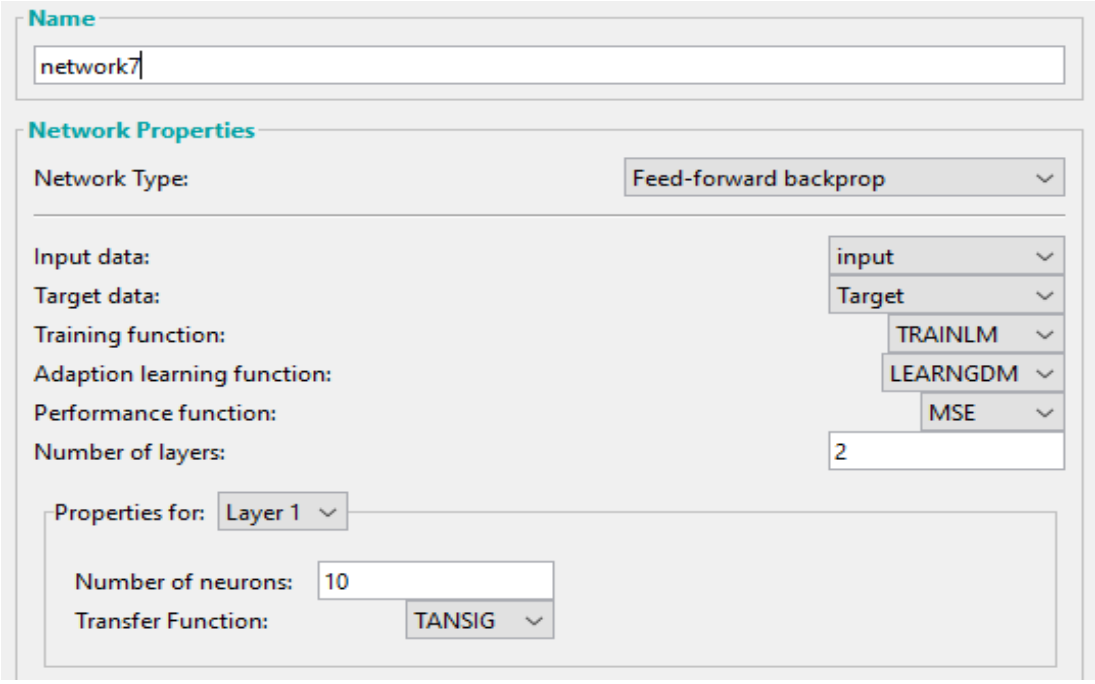


Figure 11. Network Properties

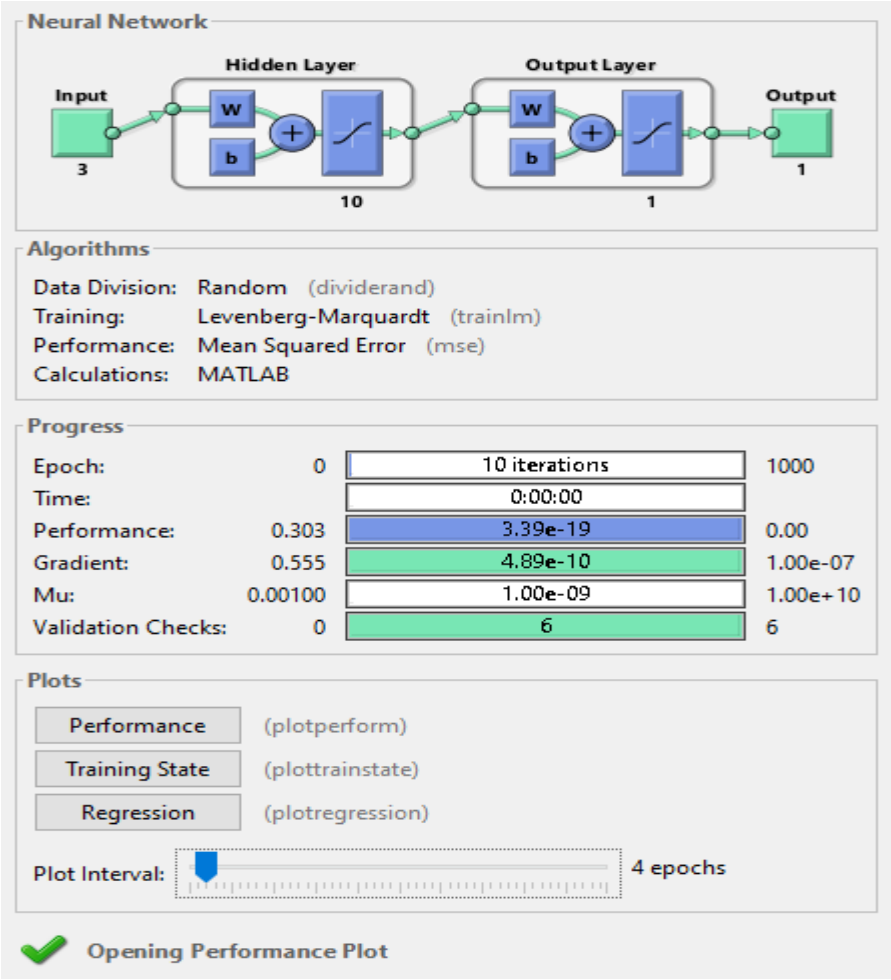


Figure 12. Model Summary for Predicting Chip Reduction Coefficient

Figure 13 shows the neural network's learning accuracy as a function of the successive training epochs with changes in MSE. The plotted trajectories reveal the learning behaviour of the training, validation, and testing subsets, with the training and validation errors exhibiting closely matched patterns throughout the optimization process. The lowest validation error identifies the most favourable network configuration before overfitting becomes a concern. Figure 13 also demonstrates the prediction accuracy by the model's capacity to reproduce minimum measured CRC values, particularly within operating conditions associated with reduced cutting forces.

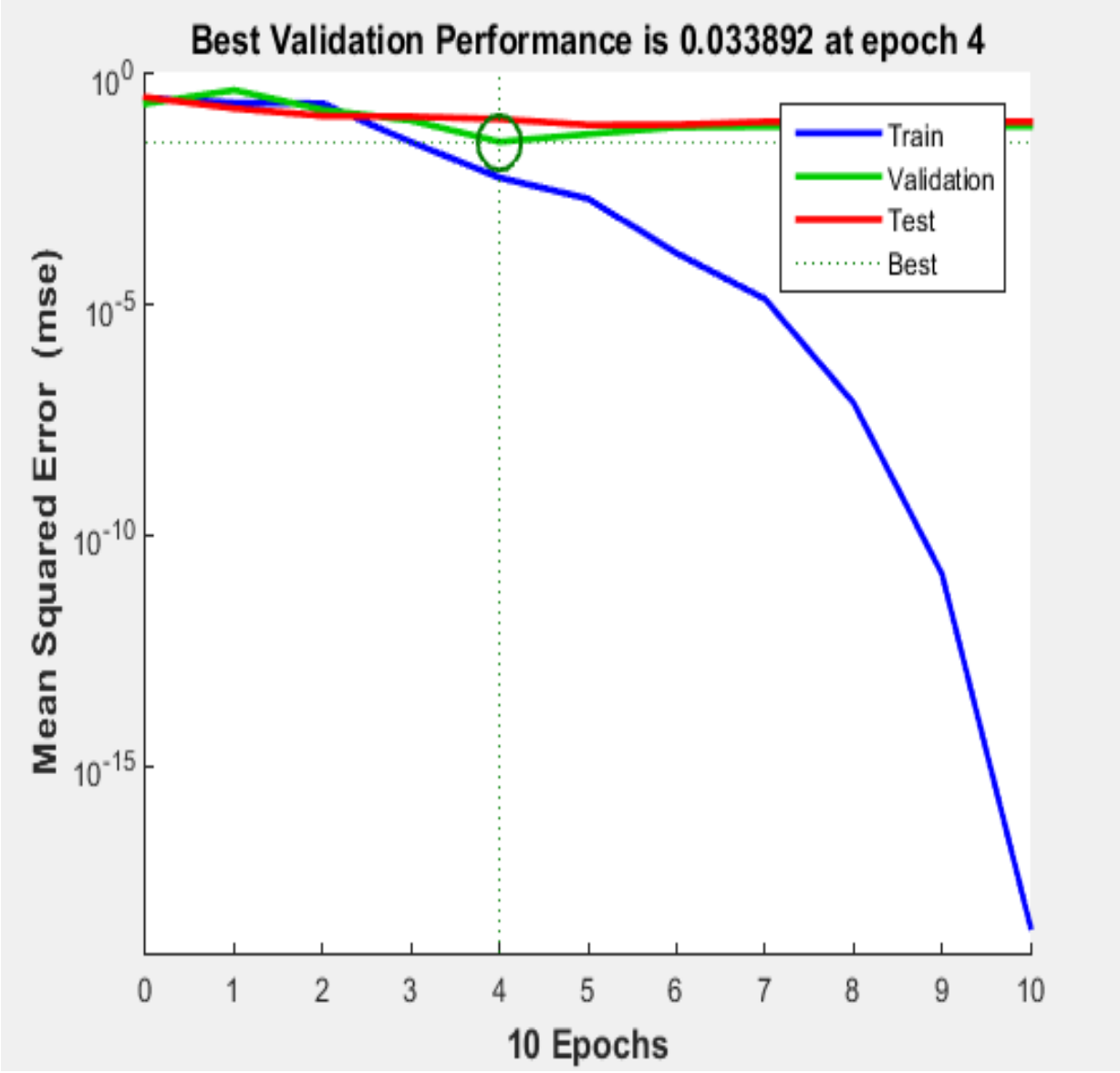


Figure 13. ANN Model Convergence Curve

Figure 14 shows the neural network's optimization behavior in predicting the CRC, with the gradient progression, Mu adjustment parameter, and validation monitoring. The declining gradient reflects progressive weight refinement across the connections linking the three machining inputs features including depth of cut, cutting speed, and feed rate; to the predicted CRC output. Validation record shows that the learning process was terminated in an appropriate manner so that the risk of overfitting to the noise in the normalized data is minimized. The training convergence and predictive performance are consistent and reliable, as confirmed by the training progression.

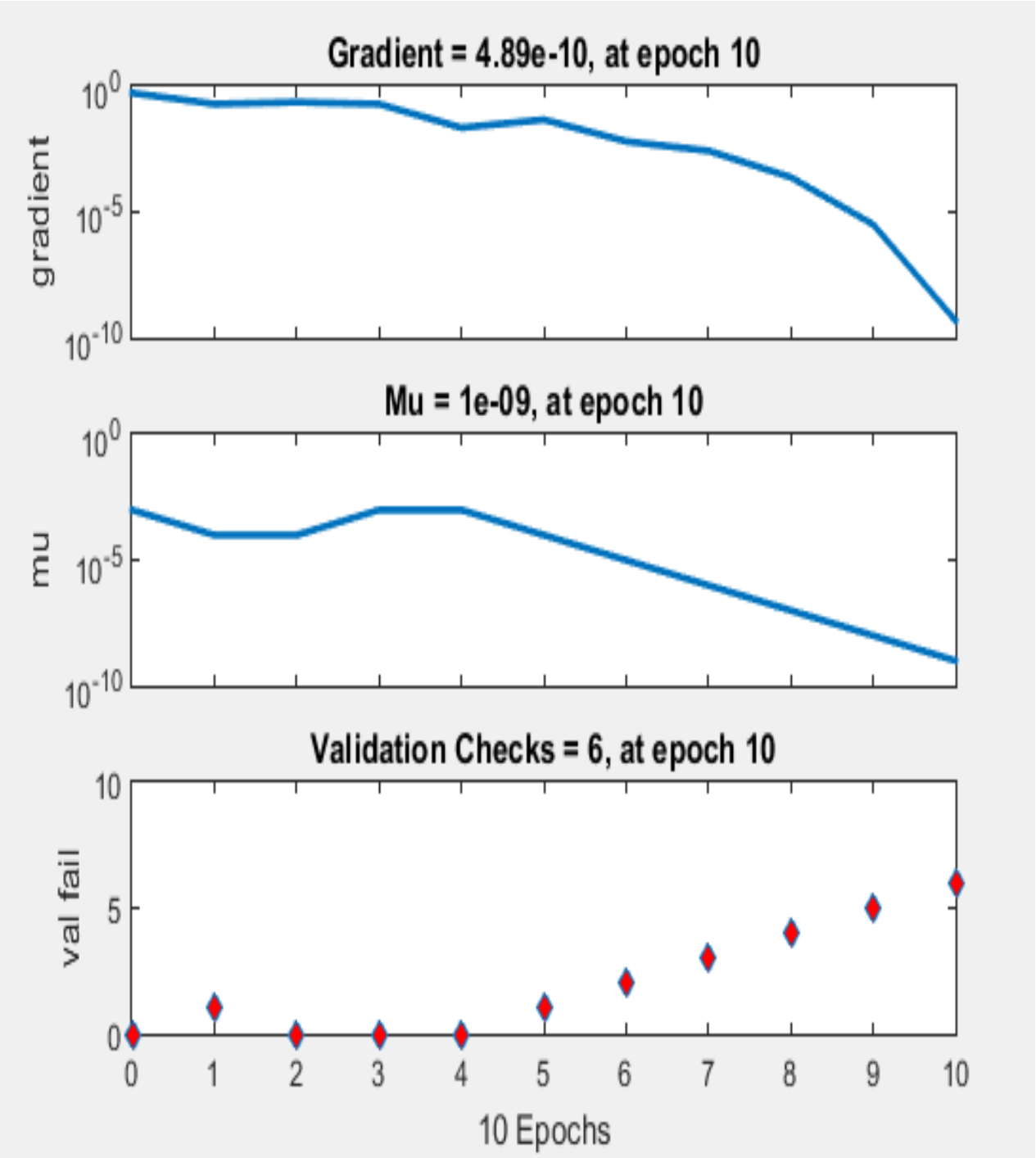


Figure 14. Neural Network Training State for Predicting Chip Reduction Coefficient

The training performance and generalization capability of the developed ANN are illustrated by the regression plots in Figure 15, covering the training, validation, and testing datasets. The scatter plots show that the predicted values of the chip reduction coefficient have a close linear relationship with the experimental values for all three sets of data, as evidenced by the degree of scatter around the regression lines. This agreement implies that the network is able to capture the variations of the response to changes in current, voltage, and gas flow rate. High correlation coefficients also illustrate the network's consistency in prediction, showing acceptable weight optimization during training, while no signs of a decrease in performance were observed that could result from unstable weight adjustments.

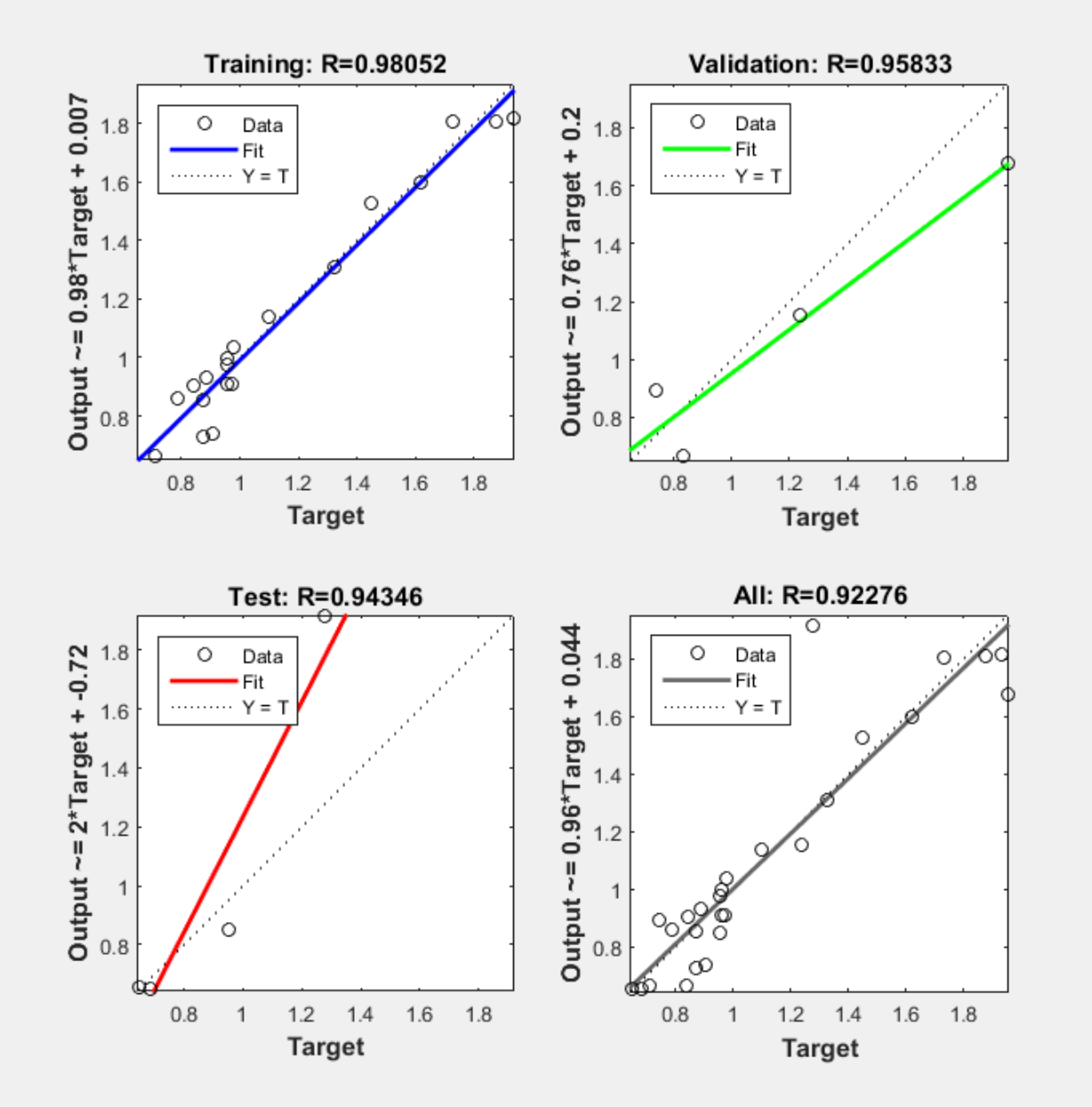


Figure 15. ANN Model Predictive Performance

4. CONCLUSION

This present study has successfully developed and validated predictive models for chip reduction coefficient during dry drilling of mild steel. The results gotten from the study shows that CRC is governed primarily by interactions, not main effects. The AC (feed rate × depth of cut) interaction is the most influential factor ($F = 60.32$, $p < 0.0001$), followed by the quadratic effect of depth of cut (C^2: $F = 87.63$, $p < 0.0001$). The quadratic RSM model provides excellent predictive capacity ($R^2 = 0.9513$, Adj. $R^2 = 0.9075$, Adeq Precision = 15.603), making it suitable for industrial implementation. The optimal CRC of 1.80833 is achieved at feed rate 0.30 mm/rev, cutting speed 146.22 m/min, and depth of cut 0.50 mm with 93.1% desirability. ANN provides acceptable prediction (R^2 = 85.15%) but is outperformed by RSM given the current dataset size. The following conclusions can be deduced from the study:

(i) The study establishes that the behaviour of chips generated during dry drilling can be systematically characterized through the chip reduction coefficient, providing a useful response for linking machining conditions with changes in chip deformation.

(ii) The comparative modelling exercise demonstrates the value of combining statistical response-surface analysis with neural-network modelling when investigating the relationship between drilling parameters and chip behaviour. The modelling approach provides both a mathematical representation of the response and an alternative data-driven means of prediction.
(iii) The optimization procedure demonstrates that the developed modelling framework can be used not only to describe chip behaviour but also to guide the selection of drilling conditions within the investigated operating range. The study contributes to predictive machining by demonstrating the applicability of CRC as a response variable for evaluating chip behaviour and assessing conditions associated with tool-breakage risk during dry drilling. The combined use of RSM, ANN modelling, and numerical optimization provides a systematic approach for characterizing the influence of drilling parameters, predicting CRC, and identifying favourable operating conditions. Future studies should experimentally validate the optimized drilling condition and further investigate the use of CRC alongside real-time sensing techniques for proactive monitoring of chip behaviour and tool-breakage conditions.

REFERENCES

[1] B. Hamadi, M. Chaour, M. lotfi Cherrad, D. Boucherma, T. Achour, M.A. Yallese, Chip formation analysis during dry turning of C45 steel, Studies in Engineering and Exact Sciences 5 (2024) e9904. https://doi.org/10.54021/seesv5n2-414.

[2] Z. Kang, Q. Guo, Z. Li, Y. He, Y. Jiang, L. Liu, Achieving precise chip control for high-end manufacturing, Sci. Rep. 16 (2026). https://doi.org/10.1038/s41598-026-43995-7.

[3] E. Shamoto, T. Hayasaka, K. Lee, Theoretical modelling and simulation of chip clogging in drilling and experimental verification, International Journal of Advanced Manufacturing Technology 141 (2025) 5853–5871. https://doi.org/10.1007/s00170-025-15602-y.

[4] A.A. Riaz, R. Muhammad, N. Ullah, G. Hussain, M. Alkahtani, W. Akram, Fuzzy logic-based prediction of drilling-induced temperatures at varying cutting conditions along with analysis of chips morphology and burrs formation, Metals (Basel). 11 (2021) 1–18. https://doi.org/10.3390/met11020277.

[5] P. Ajagol, R.N. Marigoudar, A.B. N, G.C. Manjunath Patel, M. Shettar, A. Lakshmikanthan, Multiobjective optimization of milling performance characteristics of Al 1200 SiC metal matrix composites using statistical and artificial intelligence tools, Discov. Mater. 6 (2026). https://doi.org/10.1007/s43939-026-00625-3.

[6] M.A. Khan, R. Ahmad, M.R. ul Haq, S.H.I. Jaffery, D. Zahid, Development of an energy consumption map for turning inconel 718 through coupled chip-morphology and material-deformation analysis, Sci. Rep. 16 (2026). https://doi.org/10.1038/s41598-026-52106-5.

[7] G. Prasad, C. Raghavendra Kamath, G.S. Vijay, A review on conventional and nonconventional machining of Nickel-based Nimonic superalloy, Manuf. Rev. (Les. Ulis). 10 (2023). https://doi.org/10.1051/mfreview/2023009.

[8] R.L. Virdi, A. Pal, S.S. Chatha, H.S. Sidhu, A review on minimum quantity lubrication technique application and challenges in grinding process using environment-friendly nanofluids, Journal of the Brazilian Society of Mechanical Sciences and Engineering 45 (2023). https://doi.org/10.1007/s40430-023-04159-0.

[9] P. Kawade, S. Bokade, Review of cooling techniques used in metal cutting processes, Advances in Materials and Processing Technologies 9 (2022) 1137–1182. https://doi.org/10.1080/2374068X.2022.2109668.

[10] M. Chen, R. Peng, L. Zhao, R. Chen, Y. Luo, Effects of minimum quantity lubrication strategy with internal cooling tool on machining performance in turning of nickel-based superalloy GH4169, International Journal of Advanced Manufacturing Technology 118 (2022) 3673–3689. https://doi.org/10.1007/s00170-021-08194-w.

[11] H. Sun, H. Su, Y. Jiang, A review of fundamental mechanisms, dominant failure modes, and mitigation strategies in deep-hole drilling with twist drills, International Journal of Advanced Manufacturing Technology 145 (2026) 3075–3104. https://doi.org/10.1007/s00170-026-18554-z.

[12] J. Sklenička, J. Hnátík, J. Fulemová, M. Gombár, A. Vagaská, A. Jirásko, Experimental Analysis of Effect of Machined Material on Cutting Forces during Drilling, Materials 17 (2024). https://doi.org/10.3390/ma17112775.

[13] J. Fulemová, J. Sklenička, J. Hnátík, M. Gombár, J. Sýkora, M. Povolný, A. Lukáš, Cutting Force Mechanisms in Drilling 90MnCrV8 Tool Steel: ANOVA and Theoretical Insights, Journal of Manufacturing and Materials Processing 10 (2026). https://doi.org/10.3390/jmmp10010038.

[14] C. Tao, X. Wang, B. Zhao, W. Ding, M. Xiong, J. Xu, Q. Liu, D. Xu, Y. Zhao, J. Zhu, Material removal mechanisms in ultrasonic vibration-assisted high-efficiency deep grinding γ-TiAl alloy, Chinese Journal of Aeronautics 37 (2024) 462–476. https://doi.org/10.1016/j.cja.2024.01.021.

[15] V. Mishra, N. Bharat, K. Chakraborty, V. Kumar, M.R. Choudhury, Machine learning-based model

to predict von Mises stress and chip reduction coefficient developed during dry turning of EN36C steel, Sci. Prog. 108 (2025). https://doi.org/10.1177/00368504251349973.

[16] P. Prashanth, S.S. Hiremath, Experimental and predictive modelling in dry micro-drilling of

titanium alloy using Ti–Al–N coated carbide tools, International Journal on Interactive Design and Manufacturing 17 (2023) 553–577. https://doi.org/10.1007/s12008-022-01032-7.

[17] C. Xu, S. Yao, G. Wang, Y. Wang, J. Xu, A prediction model of drilling force in CFRP internal chip removal hole drilling based on support vector regression, International Journal of Advanced Manufacturing Technology 117 (2021) 1505–1516. https://doi.org/10.1007/s00170-021-07766-0.

[18] T. Vo-Thanh, A. Le Hoang, T. Hoang Xuan, C. Nguyen Manh, Quadratic Response Surface Modeling of Surface Roughness in CBN Grinding of HARDOX 500, Vlute Journal of Science 1 (2026). https://doi.org/10.64215/temp2.

[19] O.J. Oyejide, F. Ahmad, J.I. Achebo, J.A. Eseigbe, E.E. Enakireru, F. Amadhe, K.U. Enuezie, J. Andrew, Prediction of polyurethane foam density using hybrid feature screening and comparative hyperparameter optimization of machine learning models, Knowl. Based. Syst. 353 (2026) 117217. https://doi.org/10.1016/j.knosys.2026.117217.

[20] O.J. Oyejide, F. Ahmad, S.B. Kamaruddin, R.O. Anjorin, F. Amadhe, T.B. Adeleke, J.I. Achebo, M.A. Al-fakih, Novel prediction of gasoline yield via extremely randomized trees-based algorithm optimized by particle swarm optimization, Ain Shams Engineering Journal 18 (2027) 104517. https://doi.org/10.1016/j.asej.2026.104517.

[21] S. Sunardi, A. Nur, D. Zain, Predictive modeling of surface roughness and resultant force in CNC turning of AISI H13 using optimized artificial neural networks, Disseminating Information on the Research of Mechanical Engineering-Jurnal Polimesin 24 (2026). https://doi.org/10.30811/jpl.v24i1.7558.

[22] K. Ullrich, M. von Elling, K. Gutzeit, M. Dix, M. Weigold, J.C. Aurich, R. Wertheim, I.S. Jawahir, H. Ghadbeigi, AI-based optimisation of total machining performance: A review, CIRP J. Manuf. Sci. Technol. 50 (2024) 40–54. https://doi.org/10.1016/j.cirpj.2024.01.012.

[23] T.B. Adeleke, A.O. Lawani, O.J. Oyejide, I.C. Osuizugbo, K.U. Enuezie, F. Amadhe, R.O. Anjorin, C.M. Chiejine, Firefly-optimized ensemble learning framework for accurate solar PV power forecasting, Next Research 2 (2025) 100811. https://doi.org/https://doi.org/10.1016/j.nexres.2025.100811.

[24] O.J. Oyejide, F. Ahmad, S. bin Kamaruddin, M.O. Okwu, F. Amadhe, A.T. Basit, R. Anjorin, M. Abdulmalek, Novel stack-model configuration for Merox-treated gasoline yield prediction synergized with EMMS-CFD hydrodynamic analysis, Knowl. Based. Syst. 325 (2025). https://doi.org/10.1016/j.knosys.2025.113980.

[25] M. Olaye, K.U. Enuzie, O.O. Imala, G. Boma, A.O. Lawani, Multivariate Regression Approach in Modelling Catalytic Cracking Variables of Petroleum Refining, Nigerian Journal of Engineering Science Research 8 (2025) 164–170. https://doi.org/10.5281/zenodo.17410289.

[26] M.O. Okwu, O.B. Otanocha, B.A. Edward, B.U. Oreko, J. Oyekale, O.J. Oyejide, J. Osuji, C. Maware, K. Ezekiel, O.F. Orikpete, Investigating the Accuracy of Artificial Neural Network Models in Predicting Surface Roughness in Drilling Processes, Procedia Comput. Sci. 232 (2024) 1982–1990. https://doi.org/10.1016/j.procs.2024.02.020.